INFECTION AND IMMUNITY, Sept. 2006, p. 5106–5113 Vol. 74, No. 9
0019-9567/06/$08.00+0 doi:10.1128/IAI.00376-06

Uropathogenic *Escherichia coli* Induces Extrinsic and Intrinsic Cascades To Initiate Urothelial Apoptosis

David J. Klumpp,[1,2]* Matthew T. Rycyk,[1]† Michael C. Chen,[1] Praveen Thumbikat,[1] Shomit Sengupta,[1]‡ and Anthony J. Schaeffer[1]

Departments of Urology[1] and Microbiology-Immunology,[2] Feinberg School of Medicine, Northwestern University, Chicago, Illinois 60611

Received 7 March 2006/Returned for modification 24 April 2006/Accepted 28 June 2006

A murine model of urinary tract infection identified urothelial apoptosis as a key event in the pathogenesis mediated by uropathogenic *Escherichia coli* (UPEC), yet the mechanism of this important host response is not well characterized. We employed a culture model of UPEC-urothelium interactions to examine the biochemical events associated with urothelial apoptosis induced by the UPEC strain NU14. NU14 induced DNA cleavage within 5 h that was inhibited by the broad caspase inhibitor ZVAD, and urothelial caspase 3 activity was induced within 3 h of exposure to type 1 piliated NU14 and was dependent upon interactions mediated by the type 1 pilus adhesin FimH. Flow cytometry experiments using chloromethyl-X-rosamine and Indo-1 revealed FimH-dependent mitochondrial membrane depolarization and elevated $[Ca^{2+}]_{in}$, respectively, indicating activation of the intrinsic apoptotic pathway. Consistent with this possibility, overexpression of Bcl_{XL} inhibited NU14 activation of caspase 3. Immunoblotting, caspase inhibitors, and caspase activity assays implicated both caspase 2 and caspase 8 in apoptosis, suggesting the involvement of the intrinsic and extrinsic apoptotic cascades. To reconcile the apparent activation of both extrinsic and intrinsic pathways, we examined Bid-green fluorescent protein localization and observed translocation from the cytosol to mitochondria in response to either NU14 or purified FimH. These data suggest that FimH acts as a tethered toxin of UPEC that activates caspase-dependent urothelial apoptosis via direct induction of the extrinsic pathway and that the intrinsic pathway is activated indirectly as a result of coupling by caspase 8-mediated Bid cleavage.

Urinary tract infections (UTIs) are the second most common infectious disease, following respiratory tract infections, and account for more than seven million office visits and more than one million visits to emergency departments in the United States, necessitating 100,000 hospitalizations (33). Uropathogenic *Escherichia coli* (UPEC) strains cause approximately 90% of common UTIs and differ significantly from their K-12 counterparts: UPEC genomes are about 30% larger than those of K-12 strains, and this extra genetic material encodes a variety of virulence factors that facilitate survival and growth in the host environment (16, 30). The type 1 pilus of *E. coli* is the best-characterized UPEC virulence factor, and expression of type 1 pili on the bacterial surface mediates bacterial attachment to host cells by virtue of the adhesin protein FimH, which occupies the tip of the pilus (reviewed in reference 14). The FimH adhesin possesses a lectin activity that is specific for mannosylated proteins, and this adherence is enhanced by shear stress, a property ideally suited to maintaining bacterial attachment to the urothelium during bladder voiding (35).

Rodents inoculated transurethrally with bacteria have long been used as a model for the pathogenesis of UTIs. Early studies noted that instilling UPEC into rat bladders induced small lesions due to the loss of superficial urothelial cells (8). More recently, Mulvey and colleagues explored the basis of this urothelial sloughing by instilling the archetypal cystitis isolate NU14 into mouse bladders (25). Time course electron micrographs demonstrated that adherent NU14 induced exfoliation of the superficial cells within several hours. Terminal deoxynucleotidyltransferase-mediated dUTP-biotin nick end label (TUNEL) staining of tissue sections from NU14-treated bladders revealed DNA degradation consistent with the onset of apoptosis, whereas the Δ*fimH* mutant NU14-1 failed to induce apoptosis, indicating that type 1 pili are required for urothelial apoptosis. Instilling a broad caspase inhibitor into mice was found to inhibit NU14-induced apoptosis and resulted in higher levels of bacterial colonization in the bladder. These data indicate that urothelial apoptosis is a key event in the pathogenesis of UTIs, yet the mechanism of UPEC-induced urothelial apoptosis is largely uncharacterized.

Apoptotic cascades are often classified as activating either the intrinsic or the extrinsic pathway. The extrinsic pathway is initiated by the engagement of death receptors of the TNFR superfamily (reviewed in references 10 and 27). Death receptor engagement then triggers the association of FADD and the recruitment of procaspase 8, and the resulting high local concentrations of procaspase 8 lead to self-cleavage and release of active caspase 8, which activates other caspases and cleaves cellular targets. The intrinsic apoptotic pathway is often regarded as a stress pathway that involves changes in mitochondrial physiology resulting in cytochrome *c* release, association of cytochrome *c* with APAF-1 to recruit procaspase 9, cleavage to activate caspase 9, and then activation of caspase 3 (reviewed in references 5 and 28). Like caspase 8, caspase 2 is

* Corresponding author. Mailing address: Department of Urology, Feinberg School of Medicine, Northwestern University, 303 East Chicago Avenue, Chicago, IL 60611. Phone: (312) 908-1996. Fax: (312) 908-7278. E-mail: d-klumpp@northwestern.edu.

† Present address: Reddy US Therapeutics, Norcross, GA 30071.

‡ Present address: Department of Biology, Massachusetts Institute of Technology, Cambridge, MA 02139.

considered an initiator caspase, yet caspase 2 mediates stress responses upstream of mitochondrial permeability (21).

Bacteria can induce apoptosis via secretion of various toxins (reviewed in reference 11), and *E. coli* initiates apoptosis by employing several mechanisms. For example, type 1 pili and lipopolysaccharide (LPS) have cooperative effects in the oxygen-dependent apoptosis of neutrophils that is induced by UPEC (1). In contrast, UPEC induces apoptosis of renal tubular cells through the effects of soluble toxins that activate caspase-independent apoptosis mediated by extracellular signal-regulated kinase 1/2 activation (3, 4). *E. coli* enterotoxin B induces $CD8^+$ T-cell death by caspase induction and nitric oxide pathways (31). However, despite this increased understanding of the diverse mechanisms by which *E. coli* induces apoptosis, the mechanism of FimH-mediated urothelial apoptosis remains unclear for this important event in UTI pathogenesis.

We previously developed a culture model of UPEC-induced urothelial apoptosis amenable to biochemical characterization that results in apoptosis with kinetics similar to those of the murine model (19). Here, we report characterization of the urothelial apoptotic response to UPEC. The UPEC isolate NU14 induced events in urothelial cultures that were consistent with activation of both the extrinsic and the intrinsic apoptotic pathways, with cross talk between these pathways mediated by Bid. Furthermore, these events were dependent upon binding of FimH, suggesting that FimH mediates both adherence and toxicity, acting effectively as a tethered toxin.

MATERIALS AND METHODS

Bacteria and reagents. NU14 is a type 1 piliated cystitis isolate of the *E. coli* B2 clonal group, and NU14-1 is an isogenic FimH mutant (17, 20). *E. coli* strains were cultured in Luria broth under static conditions to promote pilus expression (6), and expression was verified by mannose-sensitive hemagglutination (15). All caspase inhibitors were purchased from Biovision. FimC · H was obtained as a gift from Scott Hultgren, and purity was verified by sodium dodecyl sulfate (SDS)-polyacrylamide gel electrophoresis and Coomassie staining to confirm the predicted mobilities of FimC and FimH.

Cell culture. TEU-2 is a human urothelial cell line established previously by immortalization of primary human ureteral epithelial cultures with a retrovirus encoding the E6E7 oncoproteins of human papillomavirus type 16 (19). TEU-1 cells were similarly established for this study by immortalization of human ureteral epithelial cultures derived from an independent donor, SR22A cells were established by immortalization of primary bladder urothelial cells obtained from a biopsy specimen of a patient with interstitial cystitis, and PD07 cells were established by immortalization of urothelial cells obtained from normal pediatric bladder. All cell lines were maintained in keratinocyte serum-free medium (KSFM; Invitrogen) or Epi-Life (Cascade Biologics). Donor tissues were obtained in accordance with the guidelines of Northwestern University's Internal Review Board under the auspices of the Office for the Protection of Research Subjects.

Bacterial infections. Urothelial cultures were fed and maintained in medium lacking antibiotics for at least 12 h prior to experiments. On the day of experiments, *E. coli* strains were quantified by spectrophotometry at 595 nm, harvested by centrifugation, resuspended in phosphate-buffered saline (PBS), and added to fresh cell culture medium without antibiotics to achieve a multiplicity of infection (MOI) of 250 *E. coli* cells/urothelial cell. Infections proceeded at 37°C and 5% CO_2 for the indicated times before assays were performed. For Bid translocation experiments, an MOI of 500 was used. We previously established (19) that an MOI of 250 to 500 resulted within 5 h in pilus-dependent urothelial apoptosis that mimics the kinetics and specificity of UPEC-induced urothelial apoptosis in a murine model of UTI (24).

TUNEL assay. TEU-1 cells were cultured in LabTek chambered slides (Nunc). The medium was removed from each well and replaced with antibiotic-free KSFM containing NU14 (MOI of 250) and/or 2 μM ZVAD-FMK. Following incubation at 37°C for 5 h, cells were fixed and stained for cleaved DNA using an in situ cell death detection kit (Roche), and labeled nuclei were visualized by epifluorescence.

Caspase assays. Caspase 3 activity was measured using peptide Ac-DEVD-AFC as a specific substrate (Enzyme Systems Products). Briefly, urothelial cell lysates were made by lysis in radioimmunoprecipitation assay buffer containing phenylmethylsulfonyl fluoride. Assays were performed by adding 90 μl of cell lysate (50 to 100 μg protein) to a reaction buffer of 100 mM HEPES (pH 7.4), 0.1% CHAPS {3-[(3-cholamidopropyl)-dimethylammonio]-1-propanesulfonate}, 1% sucrose, 2 mM dithiothreitol containing 0.77 mM substrate in a total volume of 200 μl. Accumulation of specific cleavage products was monitored by fluorescence (excitation, 400 nm; emission, 505 nm) in a SPECTRAmax Gemini XS plate reader (Molecular Devices) for 60 min. Values for V_{max} were calculated using SoftMax Pro 4.0 (Molecular Devices), and caspase activities were expressed as changes (*n*-fold) by normalizing to those for untreated cultures. An initial time course experiment identified maximal caspase 3 activity at 2.5 to 3.0 h after the addition of *E. coli* (data not shown), so this time period was used in all subsequent experiments for caspase 3. Caspase 2 and 8 activities were measured similarly, except that Ac-VDVAD-AFC and Ac-Ile-Glu-Thr-Asp-AFC (Enzyme Systems Products), respectively, were employed as substrates, and an initial time course experiment revealed that exposure of urothelial cultures to bacteria for 1.5 h achieved maximal activity (data not shown). Caspase inhibitors were employed by adding the inhibitor to culture medium at a final concentration of 2 μM, according to the manufacturer's recommendation.

Caspase cleavage was assessed by immunoblotting. TEU-1 cultures were incubated with NU14 (MOI 250) for 0 to 3.0 h, cells were harvested on ice, and whole-cell extracts were prepared in radioimmunoprecipitation assay buffer containing protease inhibitor cocktail (Sigma). Protein extracts (30 μg/lane) were separated by electrophoresis through SDS-polyacrylamide (10% for caspase 8, 15% for caspase 2) and blotted to Immobilon-P (Millipore). Cleaved caspase 2 was detected using a monoclonal antibody under the conditions recommended by the manufacturer (#2244, diluted 1:1,000; Cell Signaling). Caspase 8 was detected using a monoclonal antibody as previously described (32). Following the binding of secondary antibodies conjugated to horseradish peroxidase, immunoreactivity was detected by enhanced chemiluminescence (Pierce). Blots were then stripped using Restore buffer (Pierce) and reprobed with an antibody specific for glyceraldehyde-3-phosphate dehydrogenase (GAPDH) (sc-32233; Santa Cruz) as a loading control.

Cytochrome *c* release. Urothelial cultures in 15-cm plates were treated with *E. coli* for 2.5 h in the presence or absence of 25 mM methyl α-D-mannopyranoside and washed with ice-cold PBS. Cells were harvested by scraping and centrifugation. An S-100 cytosolic fraction was prepared by lysis in hypotonic buffer: cell pellets were resuspended in 100 μl of 20 mM HEPES-KOH (pH 7.5), 250 mM sucrose, 10 mM KCl, 1.5 $MgCl_2$, 1 mM Na_2EDTA, 1 mM Na_2EGTA, 1 mM dithiothreitol, 0.1 mM phenylmethylsulfonyl fluoride, and protease inhibitor cocktail (Sigma). After incubation on ice for 15 min, cell suspensions were lysed by Dounce homogenization for 15 strokes in a 1 ml Kontes Dounce homogenizer fitted with pestle B. Centrifugation at 1,000 × *g* for 10 min at 4°C was performed to remove nuclei, and the supernatant was cleared by centrifugation at 100,000 rpm in a Beckman TL-100 ultracentrifuge. Supernatants were quantified for cytochrome *c* (1 μg each) by enzyme-linked immunosorbent assay (ELISA) according to the manufacturer's instructions (Biosource), fractionated by electrophoresis through 10% SDS-polyacrylamide gels (5 μg each), and electroblotted to Immobilon-P membrane (Millipore). Nonspecific binding was blocked by incubation of the membrane in Tris-buffered saline–Tween buffer containing 5% milk diluent (Kirkegaard), the filter was probed with anti-VDAC (PA1-954, diluted 1:1,000; Affinity BioReagents) and anti-rabbit-horseradish peroxidase (diluted 1:10,000; Amersham), and immune complexes were detected with SuperSignal West Dura reagent (Pierce).

Flow cytometry. Urothelial cultures were treated with *E. coli* for 5 h. Cells were then washed with PBS and harvested by trypsin digestion. For determining mitochondrial membrane potential, cells were resuspended in KSFM at 1×10^6/ml, MitoTracker Red chloromethyl-X-rosamine (CMXRos) (Molecular Probes) was added to 10 nM/ml with gentle mixing, and cells were incubated at 37°C and 5% CO_2 for 15 min, washed, resuspended in PBS, and immediately characterized on a Coulter EPICS XL flow cytometer. Cytosolic calcium levels were similarly characterized using ratiometric analyses of Indo-1 (Molecular Probes) at 405/485 nm. After being treated with NU14, cells were rinsed with PBS, 5 μM Indo-1 in PBS was added, cells were incubated on ice for 30 min, cell were harvested with trypsin, and cells were resuspended in PBS and immediately assayed on a Beckman Coulter Elite ESP instrument.

Bid translocation. Urothelial cells were cultured in LabTek II chambered coverslips (Nunc), and cultures were transfected with BD4EGFP-Bid (BD Clontech) using Lipofectamine 2000 (Invitrogen) according to the manufacturer's

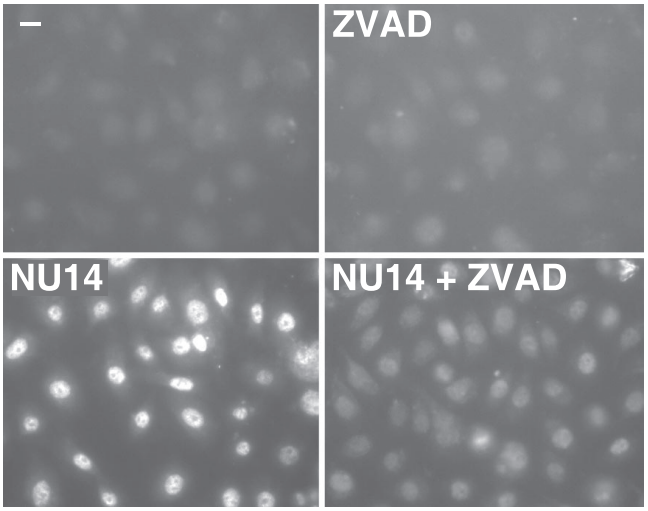

FIG. 1. Strain NU14 induces caspase-dependent urothelial apoptosis. TEU-1 cells were infected with strain NU14 at an initial MOI of 250 in the presence or absence of the broad caspase inhibitor ZVAD-FMK (ZVAD) for 5 h. Following incubation, apoptotic cells were identified by fluorescent TUNEL assay for DNA degradation. Strain NU14 induced DNA degradation in urothelial cells (lower left panel), but similar DNA degradation was blocked in cells infected with strain NU14 in the presence of ZVAD-FMK (lower right panel). Magnification, ×40. Data are representative of triplicate experiments.

instructions. Prior to the experiment, green fluorescent protein (GFP)-positive urothelial cells were identified, and the *x*, *y*, and *z* positions were set using the motorized stage of a Leica DM IRE2 inverted fluorescent microscope driven by OpenLab software (Improvision). Initial images were then captured using a Hamamatsu C4742-95-12ERG camera. NU14 was added at an initial MOI of 500, the cultures were returned to 37°C and 5% CO_2, and the GFP-positive cells were imaged repeatedly at 30-minute intervals. Following the final image capture, cultures were stained with MitoTracker Red CMXRos, according to the manufacturer's instructions, to reveal mitochondria. Cultures were then imaged in red and green channels, and color channels were merged in Photoshop (Adobe) to determine colocalization of Bid and mitochondria.

Statistics. Data are reported as means ± standard deviations. Statistical significance was determined by Student's *t* test, and data yielding *P* values of <0.05 were considered statistically significant.

RESULTS

Since a murine model of cystitis implicated caspases in the urothelial apoptotic response (25), we initially sought to demonstrate a similar role for caspase activation in our culture model of urothelial apoptotic responses to UPEC. TEU-1 ureteral urothelial cells were incubated with the type 1 piliated cystitis isolate NU14 and examined for apoptosis by TUNEL staining (Fig. 1). TUNEL-positive nuclei were prominent in cells exposed to NU14 yet were absent in untreated cells. The pancaspase inhibitor ZVAD-FMK blocked the induction of TUNEL staining in NU14-treated cultures, suggesting that caspases play a role in urothelial apoptotic responses to UPEC in culture. Thus, our urothelial model mimics a key aspect of the in vivo apoptotic response yet offers a convenient system for biochemical characterization of the apoptotic cascade.

Caspase 3 can be activated by either the intrinsic or the extrinsic apoptotic pathway, so we examined whether UPEC induced urothelial caspase 3 activity. TEU-1 cultures were treated with NU14 for 3 h, and cell lysates were assayed for caspase 3 activity with the fluorogenic substrate DEVD-AFC (Fig. 2). Caspase 3 activity in urothelial cell lysates treated with NU14 was significantly elevated 3.2-fold relative to that seen for extracts of mock-treated urothelial cultures ($P < 0.001$). Caspase 3 induction was not observed for extracts of urothelial cultures treated with NU14 in the presence of methyl α-D-mannopyranoside, a competitive inhibitor of interactions mediated by FimH, or for extracts of cultures treated with the Δ*fimH* mutant NU14-1 ($P < 0.001$). Similar results were obtained using cultures of SR22A, a bladder urothelial line, where caspase 3 activity was induced 3.4-fold and was FimH dependent ($P < 0.001$). These data indicate that the activation

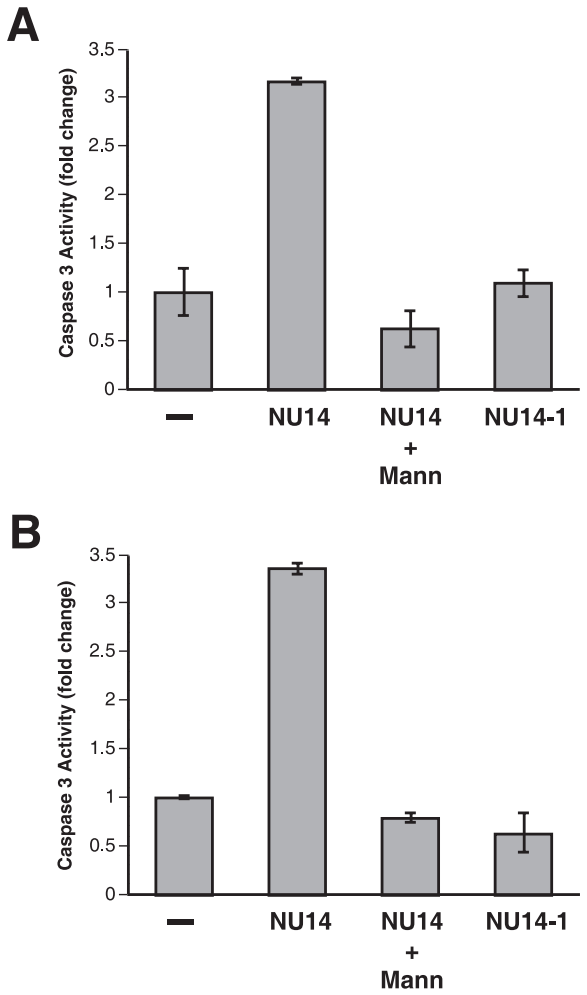

FIG. 2. Strain NU14 induces FimH-dependent caspase 3 activity. (A) TEU-1 cells were infected with strain NU14, with the Δ*fimH* mutant NU14-1, or with NU14 in the presence of 25 mM methyl α-D-mannopyranoside (Mann). All infections were performed at an initial MOI of 250, and urothelial caspase 3 enzymatic activity levels were then determined for cell extracts by cleavage of the fluorogenic substrate Ac-DEVD-AFC and compared with the activity level for extracts of untreated cultures (−). (B) The caspase 3 activity level was also determined in a similar experiment using cultures of SR22A bladder urothelial cells. Caspase 3 activity was induced in both TEU-1 and SR22A cultures by strain NU14 but was blocked by the competitive inhibitor methyl α-D-mannopyranoside or a mutation in the gene encoding FimH. Error represents the standard deviation for triplicate infections.

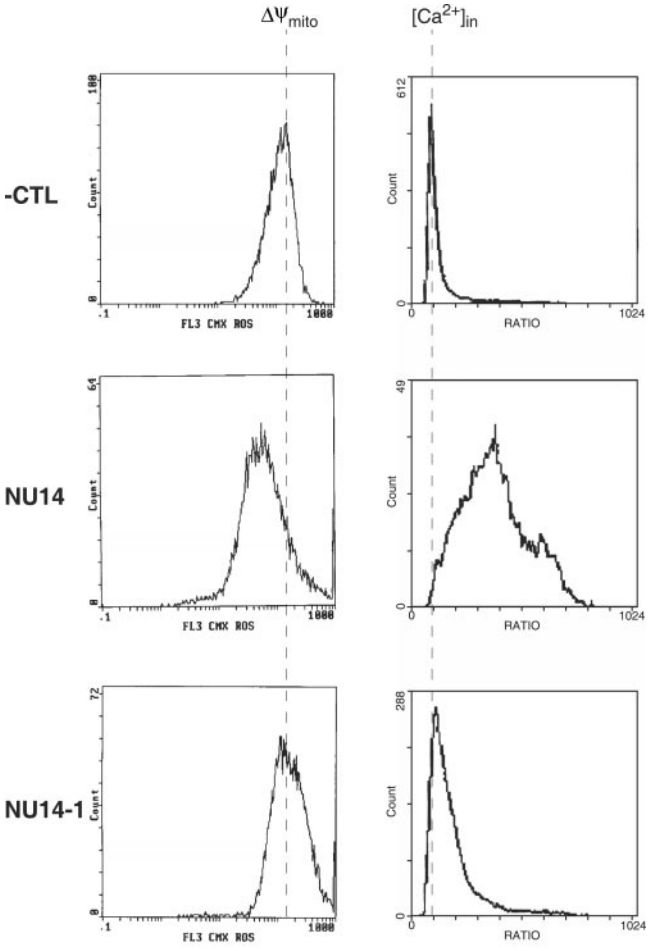

FIG. 3. Strain NU14 induces FimH-dependent mitochondrial membrane depolarization and increased cytosolic calcium. TEU-2 cultures were infected with strain NU14 or strain NU14-1 at an initial MOI of 250 for 5 h and then analyzed by flow cytometry for mitochondrial membrane potential ($\Delta\Psi_{mito}$; left panels) or cytosolic calcium ($[Ca^{2+}]_{in}$; right panels) by use of CMXRos and Indo-1, respectively. Control cultures (upper panels; −CTL) had high mitochondrial membrane potential and low cytosolic calcium, but NU14-treated cultures (middle panels) exhibited decreased mitochondrial membrane potential and increased cytosolic calcium. Cultures infected with strain NU14-1 (lower panels) were largely unaffected. Vertical dashed lines indicate the population mode of control cultures and facilitate comparison of panels within the columns. Data are representative of triplicate experiments.

of urothelial caspase 3 by the UPEC isolate NU14 is dependent upon interactions mediated by type 1 pili and is a response common to urothelial cell lines of both bladder and ureteral origin.

NU14 activation of urothelial caspase 3 suggested that UPEC-induced apoptosis may proceed via the intrinsic pathway. In a further exploration of the possible involvement of the intrinsic pathway, mitochondrial membrane potential was examined using flow cytometry to determine the fluorescence of the dye CMXRos in urothelial cultures treated with NU14 or NU14-1. CMXRos is a variant of MitoTracker Red that fluoresces only in actively respiring cells, where the dye is oxidized to the fluorescent from and sequestered in mitochondria. NU14 treatment induced mitochondrial depolarization relative to mock-treated cells, and this depolarization was not induced by treatment of urothelial cultures with NU14-1 (Fig. 3, left column). Since changes in mitochondrial physiology that occur during apoptosis are often associated with elevated cytosolic calcium (28), cytosolic Ca^{2+} levels were examined by ratiometric fluorescence of the calcium-sensitive dye Indo-1 (Fig. 3, right column). NU14 treatment resulted in a population of urothelial cells that exhibited a broad distribution of cells with elevated cytosolic Ca^{2+}, whereas both mock-treated and NU14-1-treated urothelial cells exhibited only narrow distributions of cells with relatively low calcium. The cytosolic Ca^{2+} increase was likely due to FimH alone, as opposed to acting in concert with activities of other NU14 factors, because purified FimC · H also increased cytosolic Ca^{2+} (P. Thumbikat, unpublished observations). This rise in cytosolic Ca^{2+} was inhibited by the intracellular calcium chelator BAPTA-AM [1,2-bis(*o*-aminophenoxy)ethane-*N*,*N*,*N*′,*N*′-tetraacetic acid tetra(acetoxymethyl) ester] but was not affected by incubating the cells in the presence of EGTA (data not shown), suggesting that the elevated cytosolic calcium was due to release from intracellular stores. Increased cytosolic Ca^{2+} apparently plays a role in the apoptotic response, because we found that BAPTA-AM treatment attenuates morphological changes associated with apoptosis, such as membrane blebbing (data not shown).

Mitochondrial instability results in the release of cytochrome *c*, and this cytochrome *c* may then drive caspase activation. S-100 extracts were prepared from urothelial cultures following exposure to NU14 to determine if UPEC induces the accumulation of cytochrome *c* in the cytosol. Indeed, ELISA revealed that NU14 exposure resulted in the accumulation of cytochrome *c* in the soluble fraction, and this accumulation was blocked in cultures that were treated with NU14 in the presence of a mannose analog (Fig. 4A). Immunoblotting for VDAC confirmed that cytosolic preparations were free of contaminating mitochondria, for VDAC protein was absent from S-100 fraction. Since caspase 3 can be activated either independent of or via cytochrome *c*-mediated organization of the apoptosome, we examined the role of cytochrome *c* by overexpressing Bcl_{XL} to stabilize the mitochondria. TEU-1 cultures were infected with recombinant adenoviruses encoding either Bcl_{XL} or luciferase and then subsequently infected with NU14 and assayed for induction of caspase 3 activity (Fig. 4B). Cell extracts from urothelial cultures treated with NU14 exhibited a 4.3-fold increase in caspase 3 activity relative to that seen for cell extracts of untreated cultures ($P = 0.004$), and infection with the control adenovirus encoding luciferase had no significant effect on NU14-induced caspase 3 induction ($P = 0.558$). In contrast, overexpression of Bcl_{XL} significantly reduced NU14-induced caspase 3 activity ($P = 0.02$), further supporting the involvement of mitochondria in the apoptotic response to UPEC. Bcl_{XL} overexpression did not, however, block caspase 3 entirely (44% block), suggesting the possible induction of caspase 3 activity independent of mitochondria.

To assess the role of upstream initiator caspases in the activation of caspase 3, selective inhibitors were employed to specifically block caspases 2 and 8 prior to infection with NU14. TEU-1 cultures were treated with a specific caspase inhibitor, infected with NU14, and assayed for caspase 3 activity (Fig. 5A). Interestingly, inhibitors of both caspase 2 and

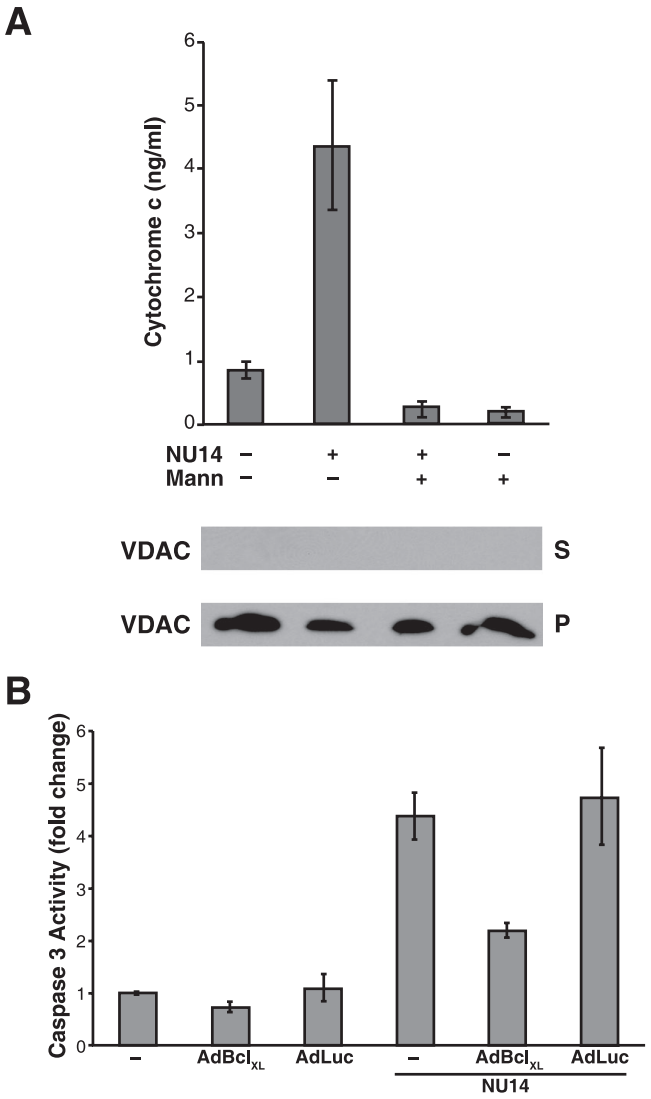

FIG. 4. Strain NU14 induces cytochrome *c* release, and caspase 3 activity is blocked by Bcl_{XL}. (A) TEU-1 cultures were infected with strain NU14 at an initial MOI of 250 for 2.5 h in the presence or absence of 25 mM methyl α-D-mannopyranoside (Mann). S-100 extracts were prepared, and supernatants were analyzed for cytosolic cytochrome *c* by ELISA. Strain NU14 induced significant accumulation of cytosolic cytochrome *c* ($P < 0.01$) that was blocked by methyl α-D-mannopyranoside ($P < 0.01$ relative to NU14 treatment alone) and not observed for untreated cultures. Immunoblotting detected VDAC protein in S-100 pellets (P) but not in S-100 soluble fractions (S). Data are representative of duplicate experiments. (B) TEU-1 cultures were infected with adenoviruses encoding luciferase (AdLuc) or Bcl_{XL} ($AdBcl_{XL}$). The following day, cultures were infected with strain NU14, and then caspase 3 activity was quantified by DEVD-AFC cleavage. Strain NU14 induced caspase 3 activity that was not induced by the adenoviruses. Adenovirus encoding Bcl_{XL} inhibited NU14-induced caspase 3 activity, whereas adenovirus encoding luciferase did not. Data are representative of triplicate experiments.

caspase 8 significantly attenuated caspase 3 induction by 73% and 64%, respectively ($P < 0.001$). To confirm the involvement of these initiator caspases, caspase 2 and 8 enzymatic activities were measured for TEU-1 cultures treated with NU14 for 1.5 h (Fig. 5B). NU14 induced a significant increase in urothelial

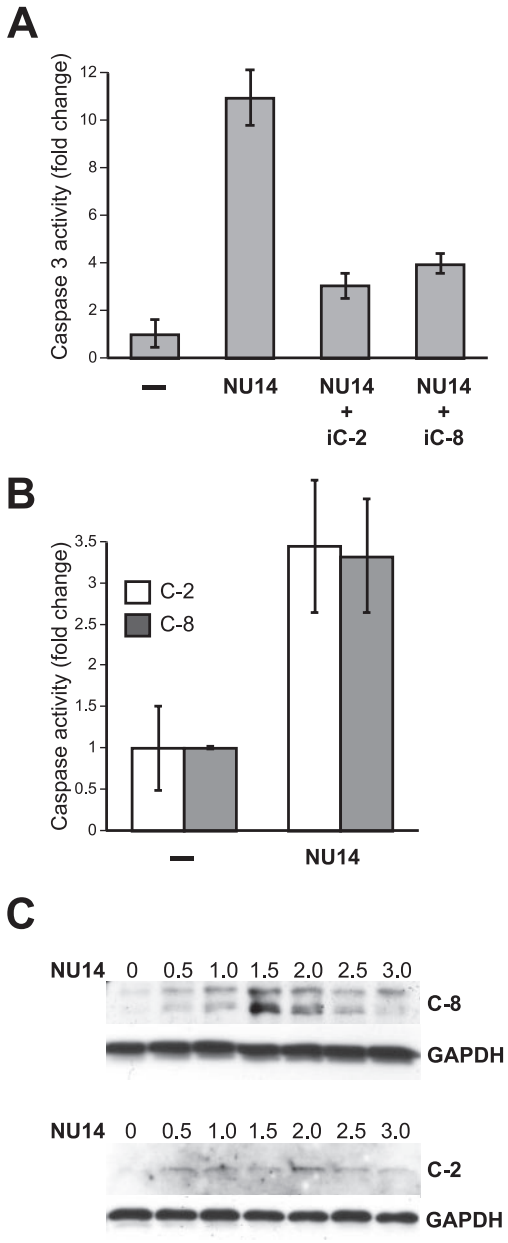

FIG. 5. Strain NU14 induces caspase 2 and caspase 8. (A) TEU-1 cultures were infected with strain NU14 at an initial MOI of 250 in the presence of specific inhibitors of caspase 2 and caspase 8 (iC-2 [z-VDVAD-FMK] and iC-8 [z-IETD-FMK], respectively). NU14-induced caspase 3 activation was largely blocked in cultures treated with the caspase 2 or caspase 8 inhibitors. (B) TEU-1 cultures were infected with strain NU14 for 1.5 h and assayed for caspase 2 (C-2) activity or caspase 8 (C-8) activity by the cleavage of the fluorogenic caspase 2 substrate Ac-VDVAD-AFC or the caspase 8 substrate Ac-IETD-AFC, respectively. NU14 induced both caspase 2 and 8 activities. (C) TEU-1 cultures were infected with strain NU14 at an initial MOI of 250. After infection for 0 to 3.0 h, whole-cell extracts were prepared and analyzed for accumulation of cleaved caspases by immunoblotting (30 μg/lane). Blotted membranes were then stripped and reprobed with an antibody specific for GAPDH as a loading control. Cleaved caspases were most abundant at 1.5 h and at 1.0 to 2.0 h (caspases 8 and 2, respectively).

caspase 2 activity (3.4-fold; $P = 0.048$), and caspase 8 activity trended toward a significant increase relative to untreated cells (3.3-fold; $P = 0.09$). The difference in kinetics of the caspase 2 and caspase 3 activations (1.5 and 2.5 h, respectively) suggests that the effects of specific caspase inhibitors are not merely due to overlapping sensitivity to peptide inhibitors. To further confirm the involvement of caspases 2 and 8, accumulation of cleaved caspases was examined by immunoblotting (Fig. 5C). Cleaved caspase 2 was most abundant at 1.0 to 2.0 h after exposure to NU14, consistent with induction of enzymatic activity. Similarly, cleaved caspase 8 was most abundant at 1.5 h, bolstering the inhibitor and activity data. These data implicate multiple initiator caspases in the urothelial apoptotic response initiated by UPEC.

Previous studies have demonstrated that cross talk exists between the extrinsic and intrinsic pathways; this cross talk results from caspase 8 cleavage of Bid and subsequent translocation of Bid to mitochondria (7, 22). To examine whether Bid translocation occurred within urothelial cells in response to UPEC, TEU-1 ureteral and PD07 bladder cultures were transfected with a plasmid encoding a Bid-GFP fusion protein, and Bid localization was assessed during infection with NU14 by live cell fluorescence microscopy (Fig. 6). Bid-GFP was diffusely distributed throughout urothelial cells in culture prior to treatment (Fig. 6A and B). However, within 90 min of NU14 treatment, Bid-GFP became concentrated in a perinuclear zone, indicating translocation (Fig. 6C and D), which was prominent after 3 h and associated with membrane blebbing in some cells (Fig. 6E and F). To determine if the perinuclear zone of concentrated Bid-GFP corresponded to the localization of mitochondria within urothelial cells, the NU14-treated urothelial cultures were then stained with MitoTracker, a dye specific for active mitochondria. The Bid-GFP was indeed concentrated in the perinuclear region enriched for mitochondria (Fig. 6G). Since the MitoTracker dye labels active mitochondria, areas which are yellow, red, and green, corresponding to mitochondria that are active with associated Bid-GFP, active without associated Bid-GFP, and inactive with associated Bid-GFP, respectively, can be seen. Similar results were obtained when staining either TEU-1 or PD07 cells (Fig. 6G and data not shown). These data are consistent with the cleavage of Bid that results from activation of the extrinsic apoptotic pathway and is known to activate the intrinsic pathway. Furthermore, these results demonstrate that ureteral and bladder urothelial cells exhibit similar responses to UPEC at the level of Bid translocation.

In addition to the data described here, our previous work and data from the murine UTI model indicate a strict dependence of urothelial apoptosis on FimH (19, 25). However, it is possible that, while it is FimH dependent, urothelial apoptosis also requires coincident signals induced by other *E. coli* factors. To assess this possibility, Bid-GFP translocation was examined for TEU-1 cells that were exposed to purified FimC·H, a complex of FimH with the stabilizing chaperone FimC (18). Like NU14, FimC·H induced translocation of Bid-GFP from a diffuse pattern to perinuclear localization (Fig. 6H and I), but the kinetics appeared accelerated. Whereas NU14 induced Bid-GFP translocation over 3 h, FimC·H-induced translocation occurred within 90 min. Membrane blebbing also occurred within 60 min in FimC·H-treated cultures, while blebbing occurred only by 3 h in response to NU14 (not shown). Despite differences in kinetics, these data suggest that FimH is both necessary and sufficient to induce urothelial apoptosis.

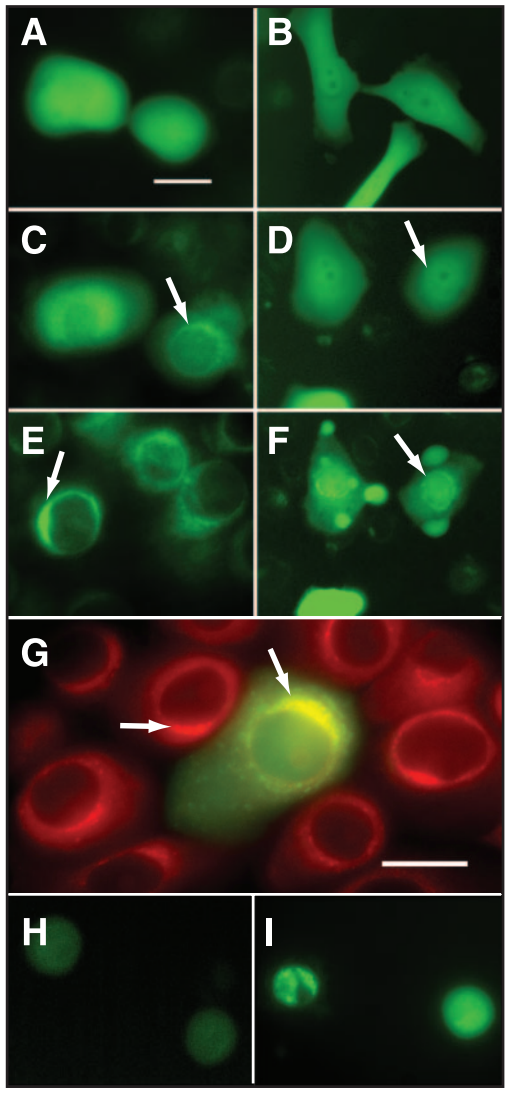

FIG. 6. Strain NU14 induces Bid translocation to mitochondria. TEU-1 cultures (A, C, and E) and SR22A cultures were transfected with BD4EGFP-Bid. After 24 h, cultures were infected with strain NU14 at an initial MOI of 500, and GFP-Bid localization was monitored via epifluorescence at 0 min (A and B), 90 min (C and D), and 180 min (E and F). Bid underwent a shift in localization within from diffuse in untreated cells (A and B) to concentrated at perinuclear sites (arrows in C to F). (G) SR22A cells were stained with MitoTracker after 180 min of exposure to NU14. Mitochondria were localized to perinuclear sites where Bid-GFP was concentrated (arrows). BD4EGFP-Bid-transfected TEU-1 cells were also exposed to 10 μg/ml FimC · H, and translocation was evident at 90 min (I) compared with the diffuse fluorescence of resting cells at 0 min (H). Scale bars, 15 μm (shown in panel A for all panels except panel G) and 10 μm (panel G).

DISCUSSION

We report that the UPEC isolate NU14 induces caspase-dependent urothelial apoptosis via activation of both extrinsic and intrinsic apoptotic pathways, and activation of these path-

ways is mediated by type 1 pili. Activation of these processes occurs within hours, with kinetics similar to those of in vivo urothelial responses observed in a murine model of UTI. These events are FimH dependent but do not depend upon specific *fimH* alleles, for *fimH* alleles expressed in an isogenic *E. coli* background (34) elicited the same level of induction of caspase 3 (data not shown). The experimental approaches reported here were optimized for the incubation times with bacteria. While potential cross talk between pathways complicates attempts to discern temporal relationships between apoptotic processes precisely, broad relationships can be inferred. Caspase 3 activation occurs at 2.5 to 3 h and is therefore upstream of DNA degradation (5 h). Similarly, the activation of the initiator caspases 2 and 8 occurs within 1.5 h, so activation of these caspases is proximal to UPEC binding, and caspase 3 lies downstream. Cytochrome *c* release and caspase 3 activation were both observed at approximately the same time, so caspase 3 activation may result from tBid-induced destabilization of mitochondria rather than directly via caspase 8. Finally, the accelerated translocation of Bid using purified FimH (FimC·H required only 60 min to complete, whereas NU14 required 180 min for completion) suggests that pilus load on urothelial cells may alter apoptosis kinetics.

Bacterial induction of apoptosis mediated by caspases is not unique to UPEC. For example, *Salmonella* induces caspase-dependent macrophage apoptosis by the secreted toxin SipB (13). Several other bacteria also induce apoptosis, including *Legionella* through the actions of *dot* (*icm*) gene products, *Shigella* through IpaB, and *Mannheimia haemolytica* through LktA (9, 36, 40). These and other examples share a common mechanism for inducing apoptosis in the host: secretion of a soluble toxin. In contrast, UPEC-induced urothelial apoptosis is strictly dependent upon the FimH molecule that is fixed to the bacterial cell surface by the pilus stalk. Therefore, FimH effectively functions as a tethered toxin, in addition to its role in adherence, indicating that FimH is multifunctional. Afa/Dr pili of diffusely adhering *E. coli* exhibit a similar activity by promoting neutrophil apoptosis (2), but P fimbriae of UPEC have not been reported to induce apoptosis. Therefore, the tethered toxin activity of type 1 pili is representative of a class of *E. coli* toxins but is not common to all *E. coli* pili.

The FimH receptor that mediates urothelial responses in our culture model is not known. Uroplakin proteins that are expressed at very high levels on the luminal bladder surface have been shown to interact with type 1 pili in vitro and in vivo (25, 38). Although we detect low-level uroplakin expression in our urothelial cultures (data not shown), high-level uroplakin expression is largely restricted to the differentiated, superficial urothelial umbrella cells that line the bladder (39). It has not been reported whether the urothelial apoptotic responses are induced by type 1 pilus interactions with uroplakins or alternative FimH receptors. We do find that urothelial apoptosis is dependent upon the expression of uroplakin III (Thumbikat et al., unpublished data), and future experiments will determine the mechanisms by which uroplakin III-mediated signals intersect with apoptotic cascades. Nevertheless, the similar kinetics of UPEC-induced apoptosis in culture and in vivo are consistent with common signaling events. Since NU14 activates caspase 8 upstream of caspase 3 in a manner consistent with death receptor signaling, this raises the intriguing possibility that FimH interactions with uroplakins induce urothelial signals that intersect with death receptor signaling.

The precise role for urothelial apoptosis in the pathogenic program of UPEC remains unclear. A murine model of pulmonary *Pseudomonas aeruginosa* infection revealed an inverse correlation between apoptosis and organ colonization (12). Similarly, a broad caspase inhibitor increased bladder colonization by NU14 in the murine model, strongly suggesting that urothelial apoptosis is a host defense mechanism whereby the bladder lining is shed and adherent bacteria are purged during voiding (25). However, NU14 was also shown to potentiate urothelial apoptosis by a mechanism involving suppression of NF-κB (19), suggesting that the apoptotic response somehow favors UPEC. *Yersinia* suppresses NF-κB by type III-mediated secretion of YopJ, and Δ*yopJ* mutants induce dramatically diminished apoptosis and systemic infection (23). In our culture model, recombinant FimH induces an apoptotic response more profound than that seen for NU14 (Thumbikat et al., unpublished data), so it is possible that UPEC strains also have the capacity to attenuate the inherent apoptotic effects of FimH and therefore utilize multiple mechanisms to modulate urothelial apoptosis. Such modulation may differentially advantage the pathogen at distinct points in the bacterial life cycle within the bladder, much like *Chlamydia* exerts both proapoptotic and antiapoptotic influences to favor host apoptosis and invasion, respectively (reviewed in reference 37). For example, UPEC establishes intracellular reservoirs in urothelial cells that support proliferation and recurrent infection (26). Although UPEC induces massive urothelial apoptosis and sloughing of superficial cells, those cells that are invaded by UPEC must necessarily remain attached to the urothelium to function as reservoirs. We speculate that signaling events initiated by UPEC adherence trigger multiple responses, and active modulation of the host response may shift the equilibrium toward apoptosis in some cells and invasion/reservoir formation in other cells.

The UPEC-induced apoptotic response described here is shared by human urothelial cell lines generated from both ureteral and bladder tissues (Fig. 2 and data not shown). Ureteral urothelial cultures have long been used as a model of bladder urothelium due to the routine access to healthy tissue from donor nephrectomies. While bladder and ureter are similar histologically, ureteral epithelium develops from the ureteric bud, whereas the bladder epithelium develops from the urogenital sinus (24), and an area of active research in the urological community is to determine whether ureteral and bladder urothelial cells are inherently different. Our data indicate that bladder and ureteral urothelial cultures respond similarly to pathogenic insult. Clinically, pyelonephritis (kidney infection) is associated with diminished ureteral peristalsis, due to the effects of LPS, that promotes urine reflux (reviewed in reference 29). Since we find that ureteral urothelial cells are similarly sensitive to the apoptotic effects of type 1 pili, it is possible that apoptosis within the ureter exacerbates the effects of LPS on ureteral peristalsis and contributes to the urine reflux that fosters retention of UPEC in the pyelonephritic kidney. Thus, understanding the mechanisms of UPEC-induced urothelial apoptosis may identify novel therapeutic targets for prevention and treatment of both cystitis and pyelonephritis.

ACKNOWLEDGMENTS

We are very grateful to Ryan Yaggie for expert assistance with immunoblotting, to Mary Paniagua for assistance in developing the flow cytometry methods, and to Steven Campbell, John Garnett, and Earl Cheng for obtaining ureter and bladder tissues. The Bcl_{XL} and luciferase adenoviruses were generously provided by Navdeep Chandel, and the caspase 8 antibody was kindly provided by Marcus Peter. Finally, we are grateful to Scott Hultgren for the gift of purified FimC·H.

This work was supported by NIDDK award R01 DK04648 (A.J.S.).

REFERENCES

1. **Blomgran, R., L. Zheng, and O. Stendahl.** 2004. Uropathogenic *Escherichia coli* triggers oxygen-dependent apoptosis in human neutrophils through the cooperative effect of type 1 fimbriae and lipopolysaccharide. Infect. Immun. **72:**4570–4578.
2. **Brest, P., F. Betis, N. Cuburu, E. Selva, M. Herrant, A. Servin, P. Auberger, and P. Hofman.** 2004. Increased rate of apoptosis and diminished phagocytic ability of human neutrophils infected with Afa/Dr diffusely adhering *Escherichia coli* strains. Infect. Immun. **72:**5741–5749.
3. **Chen, M., W. Bao, R. Aizman, P. Huang, O. Aspevall, L. E. Gustafsson, S. Ceccatelli, and G. Celsi.** 2004. Activation of extracellular signal-regulated kinase mediates apoptosis induced by uropathogenic Escherichia coli toxins via nitric oxide synthase: protective role of heme oxygenase-1. J. Infect. Dis. **190:**127–135.
4. **Chen, M., T. Jahnukainen, W. Bao, E. Dare, S. Ceccatelli, and G. Celsi.** 2003. Uropathogenic Escherichia coli toxins induce caspase-independent apoptosis in renal proximal tubular cells via ERK signaling. Am. J. Nephrol. **23:**140–151.
5. **Cory, S., and J. M. Adams.** 2002. The Bcl2 family: regulators of the cellular life-or-death switch. Nat. Rev. Cancer **2:**647–656.
6. **Duguid, J. P., and D. C. Old.** 1980. Adhesive properties of enterobacteriaceae, p. 185–217. *In* E. H. Beachey (ed.), Bacterial adherence, vol. 6. Chapman and Hall, London, United Kingdom.
7. **Fischer, B., D. Coelho, P. Dufour, J. P. Bergerat, J. M. Denis, J. Gueulette, and P. Bischoff.** 2003. Caspase 8-mediated cleavage of the pro-apoptotic BCL-2 family member BID in p53-dependent apoptosis. Biochem. Biophys. Res. Commun. **306:**516–522.
8. **Fukushi, Y., S. Irikasa, and M. Kagayama.** 1979. An electron microscopic study of the interaction between vesical epithelium and E. coli. Investig. Urol. **17:**61–68.
9. **Gao, L. Y., and Y. Abu Kwaik.** 1999. Activation of caspase 3 during *Legionella pneumophila*-induced apoptosis. Infect. Immun. **67:**4886–4894.
10. **Gaur, U., and B. B. Aggarwal.** 2003. Regulation of proliferation, survival and apoptosis by members of the TNF superfamily. Biochem. Pharmacol. **66:** 1403–1408.
11. **Grassme, H., V. Jendrossek, and E. Gulbins.** 2001. Molecular mechanisms of bacteria induced apoptosis. Apoptosis **6:**441–445.
12. **Grassme, H., S. Kirschnek, J. Riethmueller, A. Riehle, G. von Kurthy, F. Lang, M. Weller, and E. Gulbins.** 2000. CD95/CD95 ligand interactions on epithelial cells in host defense to Pseudomonas aeruginosa. Science **290:**527–530.
13. **Hersh, D., D. M. Monack, M. R. Smith, N. Ghori, S. Falkow, and A. Zychlinsky.** 1999. The Salmonella invasin SipB induces macrophage apoptosis by binding to caspase-1. Proc. Natl. Acad. Sci. USA **96:**2396–2401.
14. **Hultgren, S., S. Normark, and S. Abraham.** 1991. Chaperone-assisted assembly and molecular architecture of adhesive pili. Annu. Rev. Microbiol. **45:**383–415.
15. **Hultgren, S. J., W. R. Schwan, A. J. Schaeffer, and J. L. Duncan.** 1986. Regulation of production of type 1 pili among urinary tract isolates of *Escherichia coli*. Infect. Immun. **54:**613–620.
16. **Johnson, J. R., P. Delavari, M. Kuskowski, and A. L. Stell.** 2001. Phylogenetic distribution of extraintestinal virulence-associated traits in Escherichia coli. J. Infect. Dis. **183:**78–88.
17. **Johnson, J. R., S. J. Weissman, A. L. Stell, E. Trintchina, D. E. Dykhuizen, and E. V. Sokurenko.** 2001. Clonal and pathotypic analysis of archetypal Escherichia coli cystitis isolate NU14. J. Infect. Dis. **184:**1556–1565.
18. **Jones, C. H., J. S. Pinkner, A. V. Nicholes, L. N. Slonim, S. N. Abraham, and S. J. Hultgren.** 1993. FimC is a periplasmic PapD-like chaperone that directs assembly of type 1 pili in bacteria. Proc. Natl. Acad. Sci. USA **90:**8397–8401.
19. **Klumpp, D. J., A. C. Wieser, S. Sengupta, S. G. Forrestal, R. A. Batler, and A. J. Schaeffer.** 2001. Uropathogenic *Escherichia coli* potentiates type 1 pilus-induced apoptosis by suppressing NF-κB. Infect. Immun. **69:**6689–6695.
20. **Langermann, S., S. Palaszynski, M. Barnhart, G. Auguste, J. S. Pinkner, J. Burlein, P. Barren, S. Koenig, S. Leath, C. H. Jones, and S. J. Hultgren.** 1997. Prevention of mucosal Escherichia coli infection by FimH-adhesin-based systemic vaccination. Science **276:**607–611.
21. **Lassus, P., X. Opitz-Araya, and Y. Lazebnik.** 2002. Requirement for caspase-2 in stress-induced apoptosis before mitochondrial permeabilization. Science **297:**1352–1354.
22. **Li, H., H. Zhu, C. J. Xu, and J. Yuan.** 1998. Cleavage of BID by caspase 8 mediates the mitochondrial damage in the Fas pathway of apoptosis. Cell **94:**491–501.
23. **Monack, D. M., J. Mecsas, D. Bouley, and S. Falkow.** 1998. Yersinia-induced apoptosis in vivo aids in the establishment of a systemic infection of mice. J. Exp. Med. **188:**2127–2137.
24. **Moore, K. L., and T. V. N. Persaud.** 1998. Before we are born: essentials of embryology and birth defects, 5th ed. W. B. Saunders, Philadelphia, Pa.
25. **Mulvey, M., Y. Lopez-Boado, C. Wilson, R. Roth, W. Parks, J. Heuser, and S. Hultgren.** 1998. Induction and evasion of host defenses by type 1-piliated uropathogenic Escherichia coli. Science **282:**494–497.
26. **Mulvey, M. A., J. D. Schilling, and S. J. Hultgren.** 2001. Establishment of a persistent *Escherichia coli* reservoir during the acute phase of a bladder infection. Infect. Immun. **69:**4572–4579.
27. **Nagata, S.** 1997. Apoptosis by death factor. Cell **88:**355–365.
28. **Newmeyer, D. D., and S. Ferguson-Miller.** 2003. Mitochondria: releasing power for life and unleashing the machineries of death. Cell **112:**481–490.
29. **Roberts, J. A.** 1992. Vesicoureteral reflux and pyelonephritis in the monkey: a review. J. Urol. **148:**1721–1725.
30. **Rode, C. K., L. J. Melkerson-Watson, A. T. Johnson, and C. A. Bloch.** 1999. Type-specific contributions to chromosome size differences in *Escherichia coli*. Infect. Immun. **67:**230–236.
31. **Salmond, R. J., R. Williams, T. R. Hirst, and N. A. Williams.** 2004. The B subunit of *Escherichia coli* heat-labile enterotoxin induces both caspase-dependent and -independent cell death pathways in $CD8^+$ T cells. Infect. Immun. **72:**5850–5857.
32. **Scaffidi, C., J. P. Medema, P. H. Krammer, and M. E. Peter.** 1997. FLICE is predominantly expressed as two functionally active isoforms, caspase-8/a and caspase-8/b. J. Biol. Chem. **272:**26953–26958.
33. **Schappert, S. M.** 1999. Ambulatory care visits to physician offices, hospital outpatient departments, and emergency departments: United States, 1997. Vital Health Stat. **13**(143)**:**i–iv.
34. **Sokurenko, E. V., V. Chesnokova, R. J. Doyle, and D. L. Hasty.** 1997. Diversity of the Escherichia coli type 1 fimbrial lectin. Differential binding to mannosides and uroepithelial cells. J. Biol. Chem. **272:**17880–17886.
35. **Thomas, W. E., E. Trintchina, M. Forero, V. Vogel, and E. V. Sokurenko.** 2002. Bacterial adhesion to target cells enhanced by shear force. Cell **109:** 913–923.
36. **Thumbikat, P., T. Dileepan, M. S. Kannan, and S. K. Maheswaran.** 2005. Mechanisms underlying Mannheimia haemolytica leukotoxin-induced oncosis and apoptosis of bovine alveolar macrophages. Microb. Pathog. **38:**161–172.
37. **Weinrauch, Y., and A. Zychlinsky.** 1999. The induction of apoptosis by bacterial pathogens. Annu. Rev. Microbiol. **53:**155–187.
38. **Wu, X.-R., T.-T. Sun, and J. Medina.** 1996. In vitro binding of type 1 fimbriated Escherichia coli to uroplakins Ia and Ib: relation to urinary tract infections. Proc. Natl. Acad. Sci. USA **93:**9630–9635.
39. **Wu, X. R., J. H. Lin, T. Walz, M. Haner, J. Yu, U. Aebi, and T. T. Sun.** 1994. Mammalian uroplakins. A group of highly conserved urothelial differentiation-related membrane proteins. J. Biol. Chem. **269:**13716–13724.
40. **Zychlinsky, A., B. Kenny, R. Menard, M. C. Prevost, I. B. Holland, and P. J. Sansonetti.** 1994. IpaB mediates macrophage apoptosis induced by Shigella flexneri. Mol. Microbiol. **11:**619–627.

Editor: J. B. Bliska